

An adaptive high dimensional stochastic model representation technique for the solution of stochastic partial differential equations

Xiang Ma, Nicholas Zabaras¹

Materials Process Design and Control Laboratory, Sibley School of Mechanical and Aerospace Engineering, 101 Frank H.T. Rhodes Hall, Cornell University, Ithaca, NY 14853-3801, USA

Abstract

Recently there has been a growing interest in quantifying uncertainty in physical systems governed by stochastic partial differential equations (SPDEs). In particular, the problem involving material heterogeneity has attracted more attention due to its relevance to several applications. A high-dimensional stochastic space (large number of random variables) is often needed to accurately quantify the uncertainty of random heterogeneous media. To this end, this problem introduces significant computational challenges when using solution methods such as stochastic Galerkin or collocation methods. The aim of this paper is to utilize a new computational tool which decomposes the high-dimensional problem into several lower-dimensional sub-problems that are easy to solve and thus alleviates to some extent the *curse of dimensionality*. This method utilizes High Dimensional Model Representation (HDMR) technique in the stochastic space to represent the model output as a finite hierarchical correlated function expansion in terms of the stochastic inputs starting from lower-order to higher-order component functions. HDMR is efficient at capturing the high-dimensional input-output relationship such that the behavior for many physical systems can be modeled only by the first few lower-order terms. An adaptive version of HDMR is developed to automatically detect the important dimensions and construct higher-order terms only as a function of the important dimensions. In this paper, we also incorporate the newly developed adaptive sparse grid collocation (ASGC) method into HDMR to solve the resulting sub-problems. By integrating HDMR and ASGC, it is computationally possible to construct a low-dimensional stochastic reduced-order model of the high-dimensional stochastic problem and easily perform various statistic analysis on the output. Flow through random heterogeneous media is considered as an example to investigate the effect of the input uncertainty on the efficiency of HDMR. The cases examined show that the method provides accurate results for stochastic dimensionality as high as 500 even with large input variability. The efficiency of the proposed method is examined by comparing with Monte Carlo (MC) simulation.

1 Introduction

Over the past few decades there has been considerable interest among the scientific community in studying physical processes with stochastic inputs. These stochastic input conditions arise from external effects such as uncertainties in boundary and initial conditions as well as from inherent random material heterogeneities. Material heterogeneities are usually difficult to quantify since it is physically impossible to know the exact property at every point in the domain. In most cases, only a few statistical descriptors of the property variation or the property variation in small test regions can be experimentally determined. This limited information necessitates viewing the property variation as a random field that satisfies certain statistical properties/correlations. Several techniques, such as Karhunen-Loève (K-L) expansion [1] and model reduction methods [2,3] have been proposed to generate these stochastic input models. This naturally results in describing the physical phenomena using stochastic partial differential equations (SPDEs).

In the past decade, there has been tremendous progress in posing and solving SPDEs with the methods used usually classified into three major groups. The first group refers to sampling methods. The most traditional one is the Monte Carlo (MC) method. Its convergence rate does not depend on the number of independent input random variables. Furthermore, MC methods are very easy to implement given a working deterministic code. However, the number of realizations required to acquire good statistics is usually quite large. The second group of methods consists of moment/perturbation methods, e.g. KL-based moment-equation approach [4–6]. These methods can deal with large number of inputs. However, they are limited to small fluctuations and do not provide high-order statistics of the solution. Significant emphasis is given recently on the non-perturbative methods. The first approach in this group for quantifying uncertainty is the spectral stochastic finite element method (SSFEM) [1] based on generalized polynomial chaos expansions (gPC) [7]. In this method, we project the dependent variables of the model onto a stochastic space spanned by a set of complete orthogonal polynomials and then a Galerkin projection scheme is used to transform the original stochastic prob-

¹ Corresponding author: Fax: 607-255-1222, Email: zabaras@cornell.edu, URL: <http://mpdc.mae.cornell.edu/>

lem into a system of coupled deterministic equations which can be solved by deterministic finite element method. The gPC was successfully applied to model uncertainty propagation in random heterogenous media [8–12]. Error bounds and convergence studies [13] have shown that these methods exhibit fast convergence rates with increasing orders of expansions. Although this method can deal with large variations of the property, the coupled nature of the resulting equations for the unknown coefficients in the spectral expansion makes the solution of the stochastic problem extremely complex as the number of stochastic dimensions and/or the number of expansion terms increase, the so called *curse of dimensionality*. In fact, computational complexity of the problem increases combinatorially with the number of stochastic dimensions and the number of expansion terms. In addition, it is required to develop a stochastic simulator, which is a non-trivial task especially if the underlying ODEs/PDEs have complicated nonlinear terms. Therefore, this method is often limited to a small number of inputs (1 – 10) .

There have been recent efforts to couple the fast convergence of the Galerkin methods with the decoupled nature of MC sampling, the so called stochastic collocation method based on sparse grids [14–19]. Hereafter, this method is referred as conventional sparse grid collocation (CSGC) method. This framework represents the stochastic solution as a polynomial approximation. This interpolant is constructed via independent function calls to the deterministic problem at different interpolation points which are selected based on the Smolyak algorithm [20]. This method is also applied to model processes in random heterogenous media [2,3,21,22]. However, there are several disadvantages. As is well known, the global polynomial interpolation cannot resolve local discontinuity in the stochastic space. Its convergence rate still exhibits a logarithmic dependence on the dimension Eq. (21). For high-dimensional problems, a higher-interpolation level is required to achieve a satisfactory accuracy. However, at the same time, the number of collocation points required increases exponentially for high-dimensional problems (> 10) as shown in Fig. 1. Therefore, its computational cost becomes quickly intractable. This method is still limited to a moderate number of random variables (5 – 15). To this end, Ma and Zabaras [23] extended this methodology to adaptive sparse grid collocation (ASGC). This method utilizes local linear interpolation and uses the magnitude of the hierarchical surplus as an error indicator to detect the non-smooth region in the stochastic space and thus place automatically more points around this region. This approach results in further computational gains and guarantees that a user-defined error threshold is met. In [23], it is shown that the ASGC can successfully resolve stochastic discontinuity problems and solve stochastic elliptic problems up to 100 dimensions when the weights of each dimension are highly anisotropic and thus when the ASGC places more points only along the first few important dimensions. However, it is also shown in the paper that when the importance of each dimension weighs equally, ASGC cannot solve the problem accurately even with moderate di-

mension 21. In this case the effect of ASGC is nearly the same as of the CSGC and thus the convergence rate deteriorates. As is well known, in realistic random heterogeneous media often we deal with a very small correlation length and this results in a rather high-dimensional stochastic space with nearly the same weights along each dimension. In this case, all the previously mentioned stochastic methods are obviously not applicable.

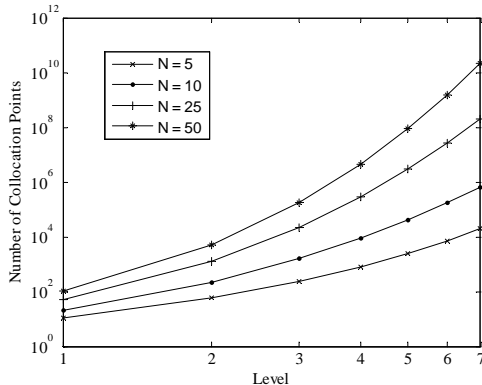


Fig. 1. Number of collocation points versus interpolation level for the conventional sparse grid collocation (CSGC) method.

These modeling issues for high-dimensional stochastic problems motivate the use of the so called High Dimensional Model Representation (HDMR) technique. It is a general set of quantitative assessment and analysis tool for capturing the high-dimensional relationships between sets of input and output model variables. It was originally developed as a methodology to create an efficient fully equivalent operational model of the original chemical systems [24–29]. It expresses the model output as an additive hierarchical superposition of correlated functions with increasing numbers of input variables, i.e. 1, 2, . . . up to the maximum number of inputs. If the correlation between higher order input variable have negligible effect upon the output, the HDMR approximation is accurate enough by using only first- or second-order component functions, which is the case for most realistic physical systems and is the ansatz that the HDMR is based upon. Depending on the way that one determines the hierarchical component functions in HDMR, there are particularly two types of HDMR: ANOVA-HDMR and CUT-HDMR [24]. ANOVA-HDMR is the same as the analysis of variance (ANOVA) decomposition used in statistics and is useful for measuring the contributions of variance of each component function to the overall variance and therefore for computing the global sensitivity [30]. It involves high-dimensional integration and thus is computational expensive. On the other hand, the CUT-HDMR expansion is a finite exact representation of the model output in the hyperplane passing through a reference point in the input variable space, which is different from gPC that has infinite terms. It only involves function evaluations at the sample points and is more computational efficient than ANOVA-HDMR. Therefore, it is our focus in this work. The model output can be considered as a function taking value over

the parameter space supported by the input variables. Therefore, it is also a multivariate function approximation (interpolation) method, which is the same idea as stochastic collocation method where the solution to the SPDEs is regarded as a stochastic function in the stochastic input space. It is thus straightforward to apply CUT-HDMR in the random space to represent the stochastic functions. The most important aspect of this method is the capability to find a way to numerically represent each component functions of HDMR. In [31], CUT-HDMR is applied to a transport model to represent the stochastic response and MC analysis is used on the obtained approximation to get statistics. However, each CUT-HDMR component function was numerically represented as a low-dimensional look-up table over its variables. To obtain an approximate value, one needs to search and interpolate in the table. In [32,33], CUT-HDMR is derived from a Taylor expansion although not mentioned explicitly in the paper and is used to find moments of the solution using the so called moment-based quadrature rule in stochastic mechanics. Later, the same author applied this method to fracture and reliability analysis, where component functions are interpolated using tensor product Lagrange polynomials and again MC analysis is used on the obtained approximation to obtain statistics [34,35]. The author in [36] also applied CUT-HDMR to reliability analysis however the interpolant is constructed through moving least squares (MLS) approximation which is only limited up to three dimensions. Most of the above applications approximate each component function on a tensor-product uniform sampling space thus they are very expensive and not very accurate implementations. In addition, all the previous applications are still limited to moderate low stochastic dimensions (< 12).

In [37], the authors have applied the same method although under the name “Anchored-ANOVA” for the computation of high-dimensional integrals using quadrature schemes with applications to finance. They also developed a dimension-adaptive version of HDMR to find the important component functions and related it with the anisotropic sparse grid method. Motivated by their work, we develop a general framework to combine the strength from both HDMR and ASGC and apply it to uncertainty quantification. We first redefine the way to compute the error indicator in the formulation of ASGC. The use of the magnitude of the hierarchical surplus as the error indicator is too sharp and may result in non-terminating algorithms. The new error indicator incorporates the information from both the basis function and the surplus. This guarantees the refinement will stop at a sufficient interpolation level. Then HDMR is used to decompose the high-dimensional stochastic problem into several lower-dimensional sub-problems. Each low-dimensional sub-problem is solved by ASGC in a *locally-adaptive* way within only related dimensions. In this way, an efficient low-dimensional stochastic reduced model is constructed and any model output in the stochastic space can be interpolated. By using ASGC, the interpolation of component functions is done efficiently by summing the corresponding hierarchical surplus and basis function as compared

with that of using a numerical table. Mean and variance can also be obtained analytically through integrating the basis functions without any MC analysis. In addition, the ASGC provides a linear combination of tensor products chosen in such a way that the interpolation error is nearly the same as for full-tensor product (numerical table) in higher dimensions. In practice, HDMR is often truncated into a lower order. However, for a very large stochastic dimension (> 100), even second-order expansion will have too many component functions. For example, 125251 component functions are needed for a second-order expansion of a 500 dimensional problem. Therefore, we need to find a way to construct only the important component functions. Motivated by the work in [37], in this paper, we also develop a dimension-adaptive version of HDMR to detect the important component functions. This is defined in two steps: First, the first-order HDMR is constructed and a weight associated with each term is defined to identify the most important dimensions. Then, higher-order components functions are constructed which consist only of these important dimensions. This method to our knowledge is the first approach which can solve high-dimensional stochastic problems by reducing the dimensions from truncation of HDMR and resolve low-regularity by local adaptivity through ASGC. It is noted here that the adaptivity in our paper is different from that used in [37]. The definition of the error indicator is not the same. The authors in [37] did not identify the important dimensions and thus there is a significant computational overhead in finding the important component functions for high-dimensional problems.

This paper is organized as follows: In the next section, the mathematical framework of stochastic ODEs/PDEs is formulated. In Section 3, the ASGC method for solving PDEs is briefly reviewed. In Section 4, we use HDMR to introduce a new method for solving SPDEs. The numerical examples are given in Section 5. Finally, concluding remarks are provided in Section 6.

2 Problem definition

In this section, we follow the notation in [23]. Let us define a complete probability space $(\Omega, \mathcal{F}, \mathcal{P})$ with sample space Ω which corresponds to the outcomes of some experiments, $\mathcal{F} \subset 2^\Omega$ is the σ -algebra of subsets in Ω and $\mathcal{P} : \mathcal{F} \rightarrow [0, 1]$ is the probability measure. Also, let us define D as a d -dimensional bounded domain $D \subset \mathbb{R}^d$ ($d = 1, 2, 3$) with boundary ∂D . We are interested in finding a stochastic function $u : \Omega \times D \rightarrow \mathbb{R}$ such that for \mathcal{P} -almost everywhere (a.e.) $\omega \in \Omega$, the following holds:

$$\mathcal{L}(\mathbf{x}, \omega; u) = g(\mathbf{x}, \omega), \quad \forall \mathbf{x} \in D, \quad (1)$$

and

$$\mathcal{B}(\mathbf{x}; u) = h(\mathbf{x}), \quad \forall \mathbf{x} \in \partial D, \quad (2)$$

where $\mathbf{x} = (x_1, \dots, x_d)$ are the coordinates in \mathbb{R}^d , \mathcal{L} is a differential operator, and \mathcal{B} is a boundary operator. The operators \mathcal{L} and \mathcal{B} and the terms g and h , can be assumed random. We assume that the boundary has sufficient regularity and that g and h are properly defined such that the problem in Eqs. (1)-(2) is well-posed for \mathcal{P} -a.e. $\omega \in \Omega$.

2.1 The finite-dimensional noise assumption and the Karhunen-Loève expansion

We employ the ‘finite-dimensional noise assumption’ [14] to approximate any second-order stochastic process with a finite-dimensional representation. One such choice is the Karhunen-Loève (K-L) expansion [1]. For example, let the force term $g(\mathbf{x}, \omega)$ be a second-order stochastic process, and its covariance function be $R(\mathbf{x}_1, \mathbf{x}_2)$, where \mathbf{x}_1 and \mathbf{x}_2 are spatial coordinates. By definition, the covariance function is real, symmetric, and positive definite. All its eigenfunctions are mutually orthonormal and form a complete set spanning the function space to which $g(\mathbf{x}, \omega)$ belongs. Then the truncated K-L expansion takes the following form:

$$g(\mathbf{x}, \omega) = \mathbb{E}[g(\mathbf{x})] + \sum_{i=1}^N \sqrt{\lambda_i} \phi_i(\mathbf{x}) Y_i(\omega), \quad (3)$$

where $\{Y_i(\omega)\}_{i=1}^N$ are uncorrelated random variables. If the process is a Gaussian process, then they are standard identically independent $N(0, 1)$ Gaussian random variables. Also, $\phi_i(\mathbf{x})$ and λ_i are the eigenfunctions and eigenvalues of the correlation function, respectively. They are the solutions of the following eigenvalue problem:

$$\int_D R(\mathbf{x}_1, \mathbf{x}_2) \phi_i(\mathbf{x}_2) d\mathbf{x}_2 = \lambda_i \phi_i(\mathbf{x}_1). \quad (4)$$

The number of terms needed to approximate a stochastic process depends on the decay rate of the eigenvalues. Generally, a higher-correlation length would lead to a rapid decay of the eigenvalues.

Following a decomposition such as the K-L expansion, the random inputs can be characterized by a set of N random variables, e.g.

$$\begin{aligned}\mathcal{L}(\mathbf{x}, \omega; u) &= \mathcal{L}(\mathbf{x}, Y_1(\omega), \dots, Y_N(\omega); u), \\ g(\mathbf{x}, \omega) &= g(\mathbf{x}, Y_1(\omega), \dots, Y_N(\omega)).\end{aligned}\tag{5}$$

Hence, by using the Doob-Dynkin lemma [39], the solution of Eqs. (1) and (2) can be described by the same set of random variables $\{Y_i(\omega)\}_{i=1}^N$, i.e.

$$u(\mathbf{x}, \omega) = u(\mathbf{x}, Y_1(\omega), \dots, Y_N(\omega)).\tag{6}$$

Thus, the use of the spectral expansion guarantees that the finite-dimensional noise assumption is satisfied and effectively reduces the infinite probability space to a N -dimensional space.

When using the K-L expansion, we here assume that we obtain a set of mutually independent random variables. The issue of non-independent random variables can be resolved by introducing an auxiliary density function [16]. In this work, we assume that $\{Y_i(\omega)\}_{i=1}^N$ are independent random variables with probability density function ρ_j . Let Γ_i be the image of Y_i . Then

$$\rho(\mathbf{Y}) = \prod_{i=1}^N \rho_i(Y_i), \quad \forall \mathbf{Y} \in \Gamma,\tag{7}$$

is the joint probability density of $\mathbf{Y} = (Y_1, \dots, Y_N)$ with support

$$\Gamma \equiv \prod_{i=1}^N \Gamma_i \in \mathbb{R}^N.\tag{8}$$

Then the problem in Eqs. (1) and (2) can be restated as: Find the stochastic function $u : \Gamma \times D \rightarrow \mathbb{R}$ such that

$$\mathcal{L}(\mathbf{x}, \mathbf{Y}; u) = g(\mathbf{x}, \mathbf{Y}), \quad (\mathbf{x}, \mathbf{Y}) \in D \times \Gamma,\tag{9}$$

subject to the corresponding boundary conditions

$$\mathcal{B}(\mathbf{x}, \mathbf{Y}; u) = h(\mathbf{x}, \mathbf{Y}), \quad (\mathbf{x}, \mathbf{Y}) \in \partial D \times \Gamma.\tag{10}$$

We assume without loss of generality that the support of the random variables Y_i is $\Gamma^i = [0, 1]$ for $i = 1, \dots, N$ and thus the bounded stochastic space is a N -hypercube $\Gamma = [0, 1]^N$, since any bounded stochastic space can always be mapped to the above hypercube.

The original infinite-dimensional stochastic problem is now restated as a finite-dimensional problem. Then we can apply any stochastic method in the random space and the resulting equations become a set of deterministic equations in the physical space that can be solved by any standard deterministic discretization technique, e.g. the finite element method. The solution to the above SPDE can be regarded as a stochastic function taking real values in the stochastic

space Γ . This nature is utilized by the stochastic collocation method which constructs the interpolant of this function in Γ through the Smolyak algorithm. However, this method still suffers from high-dimensionality. In the next few sections, a novel dimension decomposition method is introduced to transform the N -dimensional problem into several low-dimensional sub-problems.

3 Adaptive sparse grid collocation method (ASGC)

In this section, we briefly review the development of the ASGC strategy. For more details, the interested reader is referred to [23].

The basic idea of this method is to have a finite element approximation for the spatial domain and approximate the multi-dimensional stochastic space Γ using interpolating functions on a set of collocation points $\{\mathbf{Y}_i\}_{i=1}^k \in \Gamma$. Suppose we can find a finite element approximate solution u to the deterministic solution of the problem in Eq. (9), we are then interested in constructing an interpolant of u by using linear combinations of the solutions $u(\cdot, \mathbf{Y}_i)$. The interpolation is constructed by using the so called sparse grid interpolation method based on the Smolyak algorithm [20].

3.1 Smolyak algorithm

The Smolyak algorithm provides a way to construct interpolation functions based on a minimal number of points in multi-dimensional space.

Let us consider a smooth function $f : [0, 1]^N \rightarrow \mathbb{R}$. In the 1D case ($N = 1$), we consider the following interpolation formula to approximate f :

$$\mathcal{U}^i(f) = \sum_{j=1}^{k_i} f(Y_j^i) \cdot a_j^i, \quad (11)$$

with the set of support nodes $X^i = \{Y_j^i \mid Y_j^i \in [0, 1] \text{ for } j = 1, 2, \dots, k_i\}$, where $i \in \mathbb{N}$, $a_j^i \equiv a_j(Y_j^i) \in C([0, 1])$ are the interpolation nodal basis functions, and k_i is the number of elements of the set X^i . In the context of incorporating adaptivity, we have utilized the Newton-Cotes grid using equidistant support nodes [23]. The number of nodes is defined as $k_i = 1$, if $i = 1$; else $k_i = 2^{i-1} + 1$. Then the support nodes are

$$Y_j^i = \begin{cases} \frac{j-1}{k_i-1}, & \text{for } j = 1, \dots, k_i, \text{ if } k_i > 1, \\ 0.5, & \text{for } j = 1, \text{ if } k_i = 1. \end{cases} \quad (12)$$

By using equidistant nodes, it is easy to refine the grid locally. Furthermore, by using the linear hat function as the univariate nodal basis function one ensures a local support [23] that can resolve discontinuities in the stochastic space. The piecewise linear basis functions can be defined as $a_1^1 = 1$, for $i = 1$, and

$$a_j^i = \begin{cases} 1 - (k_i - 1) \cdot |Y - Y_j^i|, & \text{if } |Y - Y_j^i| < 1/(k_i - 1), \\ 0, & \text{otherwise,} \end{cases} \quad (13)$$

for $i > 1$ and $j = 1, \dots, k_i$.

Using the nested property ($X^i \subset X^{i+1}$) of the grid points, we can rewrite Eq. (11) in a hierarchical fashion, since \mathcal{U}^i can exactly represent \mathcal{U}^{i-1} , i.e., $\mathcal{U}^{i-1}(f) = \mathcal{U}^i(\mathcal{U}^{i-1}(f))$. We define $\Delta^i(f) = \mathcal{U}^i(f) - \mathcal{U}^{i-1}(f)$. Then, we can derive [23]

$$\mathcal{U}^i(f) = \sum_{m=1}^i \Delta^m(f), \quad (14)$$

where

$$\Delta^i(f) = \sum_{j=1}^{k_\Delta^i} a_j^i \cdot \underbrace{(f(Y_j^i) - \mathcal{U}^{i-1}(f)(Y_j^i))}_{w_j^i}. \quad (15)$$

Here, the index i denotes the hierarchical level. With increasing level, new support nodes are added to the interpolant. These new support nodes are given by $X_\Delta^i = X^i \setminus X^{i-1}$. Clearly, X_Δ^i has $k_\Delta^i = k_i - k_{i-1}$ points, since $X_{i-1} \subset X_i$. For simplicity, we consecutively numbered the elements in X_Δ^i , and denoting the j -th point of X_Δ^i as Y_j^i [23].

In the multivariate case ($N > 1$), the tensor product formulae are defined as

$$(\mathcal{U}^{i_1} \otimes \dots \otimes \mathcal{U}^{i_N})(f) = \sum_{j_1=1}^{k_1} \dots \sum_{j_N=1}^{k_N} f(Y_{j_1}^{i_1}, \dots, Y_{j_N}^{i_N}) \cdot (a_{j_1}^{i_1} \otimes \dots \otimes a_{j_N}^{i_N}), \quad (16)$$

which serve as building blocks for the Smolyak algorithm. The N -dimensional multilinear basis functions can be defined as $a_{\mathbf{j}}^{\mathbf{i}}(\mathbf{Y}) := a_{j_1}^{i_1} \otimes \dots \otimes a_{j_N}^{i_N} = \prod_{p=1}^N a_{j_p}^{i_p}$, where the multi-index $\mathbf{i} = (i_1, \dots, i_N) \in \mathbb{N}^N$ and the multi-index $\mathbf{j} = (j_1, \dots, j_N) \in \mathbb{N}^N$. Here $i_k, k = 1, \dots, N$, is the the level of interpolation

along the k -th direction and j_k , $k = 1, \dots, N$, denotes the location of a given support node in k -th dimension. Furthermore, through a new multi-index set

$$B_{\mathbf{i}} := \left\{ \mathbf{j} \in \mathbb{N}^N : m_{j_p}^{i_p} \in X_{\Delta}^{i_p} \text{ for } j_p = 1, \dots, k_{\Delta}^{i_p}, p = 1, \dots, N \right\}, \quad (17)$$

we can define the *hierarchical basis* as $\{a_{\mathbf{j}}^{\mathbf{i}} : \mathbf{j} \in B_{\mathbf{p}}, \mathbf{p} \leq \mathbf{i}\}$.

With $\mathcal{U}^0 = 0$, $\|\mathbf{i}\| = i_1 + \dots + i_N$, the sparse interpolant $A_{q,N}$, where q is the depth of sparse grid interpolation ($q \geq 0, q \in \mathbb{N}_0$) and N is the number of stochastic dimensions, is given by the Smolyak algorithm as

$$\mathcal{A}_{q,N}(f) = \sum_{\|\mathbf{i}\| \leq N+q} \left(\Delta^{i_1} \otimes \dots \otimes \Delta^{i_N} \right). \quad (18)$$

Analogously to the univariate case Eq. (14), the above equation can be rewritten explicitly in terms of hierarchical surpluses and basis functions as

$$\begin{aligned} \mathcal{A}_{q,N}(f) = \sum_{\|\mathbf{i}\| \leq N+q} \sum_{\mathbf{j} \in B_{\mathbf{i}}} \underbrace{\left(a_{j_1}^{i_1} \otimes \dots \otimes a_{j_N}^{i_N} \right)}_{a_{\mathbf{j}}^{\mathbf{i}}} \\ \cdot \underbrace{\left(f(Y_{j_1}^{i_1}, \dots, Y_{j_N}^{i_N}) - \mathcal{A}_{q-1,N}(f)(Y_{j_1}^{i_1}, \dots, Y_{j_N}^{i_N}) \right)}_{w_{\mathbf{j}}^{\mathbf{i}}}. \end{aligned} \quad (19)$$

Here, we define $w_{\mathbf{j}}^{\mathbf{i}}$ as the hierarchical surplus, which is just the difference between the function value at the current point and interpolation value from the coarser grid. The hierarchical surplus is a natural candidate for error control and implementation of adaptivity. However, this error indicator is too sharp and may result in a non-terminating algorithm. We will define a new error indicator in the following section.

For $f \in F_N$, where

$$F_N := \left\{ f : [0, 1]^N \rightarrow \mathbb{R}, D^{\|\mathbf{m}\|} f \text{ continues}, m_i \leq 2, \forall i \right\}, \quad (20)$$

with $\mathbf{m} \in \mathbb{N}_0^N$, the interpolation error in the maximum norm is given by [23]

$$\|f - A_{q,N}(f)\|_{\infty} = \mathcal{O} \left(M^{-2} |\log_2 M|^{3(N-1)} \right), \quad (21)$$

where M is the number of collocation points.

3.2 Definition of the error indicator

Any function $f \in \Gamma$ can now be approximated by the following reduced form from Eq. (19):

$$f(\mathbf{x}, \mathbf{Y}) = \sum_{\|\mathbf{i}\| \leq N+q} \sum_{\mathbf{j} \in B_{\mathbf{i}}} w_{\mathbf{j}}^{\mathbf{i}}(\mathbf{x}) \cdot a_{\mathbf{j}}^{\mathbf{i}}(\mathbf{Y}). \quad (22)$$

The mean of the random solution can be evaluated as follows:

$$\mathbb{E}[f(\mathbf{x})] = \sum_{\|\mathbf{i}\| \leq N+q} \sum_{\mathbf{j} \in B_{\mathbf{i}}} w_{\mathbf{j}}^{\mathbf{i}}(\mathbf{x}) \cdot \int_{\Gamma} a_{\mathbf{j}}^{\mathbf{i}}(\mathbf{Y}) d\mathbf{Y}, \quad (23)$$

where the probability density function $\rho(\mathbf{Y})$ is 1 since the stochastic space is a unit hypercube $[0, 1]^N$. The 1D integral can be evaluated analytically:

$$\int_0^1 a_j^i(Y) dY = \begin{cases} 1, & \text{if } i = 1, \\ \frac{1}{4}, & \text{if } i = 2, \\ 2^{1-i}, & \text{otherwise.} \end{cases} \quad (24)$$

Since the random variables are assumed independent of each other, the value of the multi-dimensional integral is simply the product of the 1D integrals. Denoting $\int_{\Gamma} a_{\mathbf{j}}^{\mathbf{i}}(\mathbf{Y}) d\mathbf{Y} = I_{\mathbf{j}}^{\mathbf{i}}$, we can rewrite Eq. (23) as

$$\mathbb{E}_q[f(\mathbf{x})] = \sum_{\|\mathbf{i}\| \leq N+q} \sum_{\mathbf{j} \in B_{\mathbf{i}}} w_{\mathbf{j}}^{\mathbf{i}}(\mathbf{x}) \cdot I_{\mathbf{j}}^{\mathbf{i}}. \quad (25)$$

We now define the error indicator as follows:

$$\gamma_{\mathbf{j}}^{\mathbf{i}} = \frac{\|w_{\mathbf{j}}^{\mathbf{i}}(\mathbf{x}) \cdot I_{\mathbf{j}}^{\mathbf{i}}\|_{L_2}}{\|\mathbb{E}_{\|\mathbf{i}\| \leq N-1}\|_{L_2}}. \quad (26)$$

This error indicator measures the contribution of each term in Eq. (25) to the integration value (mean) relative to the overall integration value computed from the previous interpolation level. In addition to the surpluses, it also incorporates information from the basis functions. This makes the error $\gamma_{\mathbf{j}}^{\mathbf{i}}$ to decrease to a sufficient small value for a large interpolation level according to Eq. (24). Therefore, for a reasonable error threshold, this error indicator guarantees that the refinement would stop at a certain interpolation level.

3.3 Adaptive sparse grid interpolation

Following [23], we set some notation first. The 1D equidistant points of the sparse grid can be considered as a tree-like data structure as shown in Fig. 2. We can consider the interpolation level of a grid point Y as the depth of the tree. Denote the father of a grid point as $F(Y)$, where the father of the root 0.5 is itself, i.e., $F(0.5) = 0.5$.

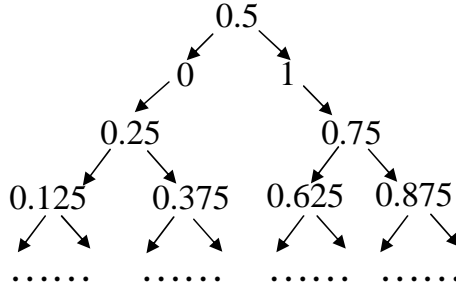


Fig. 2. 1D tree-like structure of the sparse grid.

We denote the sons of a grid point $\mathbf{Y} = (Y_1, \dots, Y_N)$ by

$$\text{Sons}(\mathbf{Y}) = \left\{ \mathbf{S} = (S_1, S_2, \dots, S_N) \mid \left(F(S_1), S_2, \dots, S_N \right) = \mathbf{Y}, \text{ or} \right. \\ \left. \left(S_1, F(S_2), \dots, S_N \right) = \mathbf{Y}, \dots, \left(S_1, S_2, \dots, F(S_N) \right) = \mathbf{Y} \right\}. \quad (27)$$

From this definition, it is noted that, in general, for each grid point there are two sons in each dimension, therefore, for a grid point in a N -dimensional stochastic space, there are $2N$ sons. It is also noted that, the sons are also the *neighbor points* of the father. The neighbor points are just the support nodes of the hierarchical basis functions in the next interpolation level [23]. By adding the neighbor points, we actually add the support nodes from the next interpolation level, i.e., we perform interpolation from level $\|\mathbf{i}\|$ to level $\|\mathbf{i}\| + 1$. Therefore, in this way, we refine the grid locally while not violating the developments of the Smolyak algorithm Eq. (19).

The basic idea here is to use the error indicator $\gamma_j^{\mathbf{i}}$ to detect the smoothness of the solution and refine the hierarchical basis functions $a_j^{\mathbf{i}}$ whose magnitude of satisfies $\gamma_j^{\mathbf{i}} \geq \varepsilon$. If this criterion is satisfied, we simply add the $2N$ neighbor points of the current point from Eq. (27) to the sparse grid. Therefore, let $\varepsilon > 0$ be the parameter for the adaptive refinement threshold. We propose the iterative refinement Algorithm 1 beginning with a coarsest adaptive sparse grid $\mathcal{G}_{N,N}$, i.e., we begin with the N -dimensional multi-index $\mathbf{i} = (1, \dots, 1)$, which is just the point $(0.5, \dots, 0.5)$.

It is noted here that by letting $\varepsilon = 0$, the algorithm reduces to the conventional sparse grid collocation (CSGC) method.

Algorithm 1 Adaptive sparse grid interpolation

Set level of Smolyak construction $q = 0$.

Construct the first level adaptive sparse grid $\mathcal{G}_{N,N}$.

- Calculate the function value at the point $(0.5, \dots, 0.5)$.
- Generate the $2N$ neighbor points and add them to the active index set.
- Set $q = q + 1$.

while $q \leq q_{max}$ and the active index set is not empty **do**

- Copy the points in the active index set to an old index set and clear the active index set.
- Calculate in parallel the hierarchical surplus of each point in the old index set according to

$$w_j^i = f(Y_{j_1}^{i_1}, \dots, Y_{j_N}^{i_N}) - \mathcal{A}_{q-1,N}(f)(Y_{j_1}^{i_1}, \dots, Y_{j_N}^{i_N}).$$

Here, we use all of the existing collocation points in the current adaptive sparse grid $\mathcal{G}_{N+q-1,N}$. This allows us to evaluate the surplus for each point from the old index set in parallel.

- For each point in the old index set, if $\gamma_j^i \geq \varepsilon$
 - Generate $2N$ neighbor points of the current active point.
 - Add them to the active index set.
- Add the points in the old index set to the existing adaptive sparse grid $\mathcal{G}_{q-1,N}$. Now the adaptive sparse grid becomes $\mathcal{G}_{q,N}$.
- $q = q + 1$.

end while

4 High dimensional model representations (HDMR)

In this section, the basic concepts of HDMR are introduced following closely the notation in [24,25,29,37]. For a detailed description of the theory applied to deterministic systems, the interesting reader may refer to [25].

Let $f(\mathbf{Y})$ be a real valued smooth multivariate stochastic function : $\mathbb{R}^N \rightarrow \mathbb{R}$. Here, it is noted that $f(\mathbf{Y})$ may be also a function of physical coordinate, $f(\mathbf{Y}, \mathbf{x})$. From now on, we will omit \mathbf{x} to simplify the notation. HDMR represents $f(\mathbf{Y})$ as a finite hierarchical correlated function expansion in terms of the input variables as [24,25,29]

$$f(\mathbf{Y}) = f_0 + \sum_{s=1}^N \sum_{i_1 < \dots < i_s} f_{i_1 \dots i_s}(Y_{i_1}, \dots, Y_{i_s}), \quad (28)$$

where the interior sum is over all sets of s integers i_1, \dots, i_s , that satisfy $1 \leq i_1 < i_s \leq N$. This relation means that

$$\begin{aligned}
f(\mathbf{Y}) = & f_0 + \sum_{i=1}^N f_i(Y_i) + \sum_{1 \leq i_1 < i_2 \leq N} f_{i_1 i_2}(Y_{i_1}, Y_{i_2}) + \cdots \\
& + \sum_{1 \leq i_1 < \cdots < i_s \leq N} f_{i_1 \cdots i_s}(Y_{i_1}, \dots, Y_{i_s}) + \cdots + f_{12 \cdots N}(Y_1, \dots, Y_N). \quad (29)
\end{aligned}$$

Here, f_0 is the zeroth-order component function which is a constant denoting the mean effect. The first-order component function $f_i(Y_i)$ is a univariate function which represents individual contributions to the output $f(\mathbf{Y})$. It is noted that $f_i(Y_i)$ is general a nonlinear function. The second-order component function $f_{i_1 i_2}(Y_{i_1}, Y_{i_2})$ is a bivariate function which describes the interactive effects of variables Y_{i_1} and Y_{i_2} acting together upon the output $f(\mathbf{Y})$. The higher-order terms reflect the cooperative effects of increasing number of input variables acting together to impact f . The s -th order component function $f_{i_1 \cdots i_s}(Y_{i_1}, \dots, Y_{i_s})$ is a s -dimensional function. The last term $f_{12 \cdots N}(Y_1, \dots, Y_N)$ gives any residual dependence of all input variables cooperatively locked together to affect the output $f(\mathbf{Y})$ [24,25]. Once all the component functions are suitably determined, then the HDMR can be used as a computationally efficient reduced-order model for evaluating the output. This is the same idea as the stochastic collocation method where we also obtain an approximate representation of $f(\mathbf{Y})$.

Equation (28) is often written in a more compact notation [37] as follows:

$$f(\mathbf{Y}) = \sum_{\mathbf{u} \subseteq \mathcal{D}} f_{\mathbf{u}}(\mathbf{Y}_{\mathbf{u}}), \quad (30)$$

for a given set $\mathbf{u} \subseteq \mathcal{D}$, where $\mathcal{D} := \{1, \dots, N\}$ denotes the set of coordinate indices and $f_{\emptyset}(\mathbf{Y}_{\emptyset}) = f_0$. Here, $\mathbf{Y}_{\mathbf{u}}$ denotes the $|\mathbf{u}|$ -dimensional vector containing those components of \mathbf{Y} whose indices belong to the set \mathbf{u} , where $|\mathbf{u}|$ is the cardinality of the corresponding set \mathbf{u} , i.e. $\mathbf{Y}_{\mathbf{u}} = (Y_i)_{i \in \mathbf{u}}$. For example, if $\mathbf{u} = \{1, 3, 5\}$, then $|\mathbf{u}| = 3$ and $f_{\mathbf{u}}(\mathbf{Y}_{\mathbf{u}})$ implies $f_{135}(Y_1, Y_3, Y_5)$.

The component functions $f_{\mathbf{u}}(\mathbf{Y}_{\mathbf{u}})$ can be derived by minimizing the error functional [24,25]:

$$\int_{\Gamma} \left[f(\mathbf{Y}) - f_0 - \sum_{i=1}^N f_i(Y_i) - \cdots - \sum_{i_1 < \cdots < i_s} f_{i_1 \cdots i_s}(Y_{i_1}, \dots, Y_{i_s}) \right]^2 d\mu(\mathbf{Y}) \quad (31)$$

where $0 \leq s \leq N$.

The measure $d\mu$ determines the particular form of the error functional and of the component functions. The measure μ induces the projection operator

$P_{\mathbf{u}} : \Gamma^N \rightarrow \Gamma^{|\mathbf{u}|}$ by [25]

$$P_{\mathbf{u}}f(\mathbf{Y}_{\mathbf{u}}) := \int_{\Gamma^{N-|\mathbf{u}|}} f(\mathbf{Y}) d\mu_{\mathcal{D}\setminus\mathbf{u}}(\mathbf{Y}), \quad (32)$$

where $d\mu_{\mathcal{D}\setminus\mathbf{u}}(\mathbf{Y}) := \prod_{i \notin \mathbf{u}} d\mu_i(Y_i)$.

Therefore, the 2^N terms $f_{\mathbf{u}}$ can be recursively defined by [24]

$$f_{\mathbf{u}}(\mathbf{Y}_{\mathbf{u}}) := P_{\mathbf{u}}f(\mathbf{Y}_{\mathbf{u}}) - \sum_{\mathbf{v} \subsetneq \mathbf{u}} f_{\mathbf{v}}(\mathbf{Y}_{\mathbf{v}}), \quad (33)$$

and can also be given explicitly by [38]

$$f_{\mathbf{u}}(\mathbf{Y}_{\mathbf{u}}) := \sum_{\mathbf{v} \subseteq \mathbf{u}} (-1)^{|\mathbf{u}|-|\mathbf{v}|} P_{\mathbf{v}}f(\mathbf{Y}_{\mathbf{v}}). \quad (34)$$

This formulation is particularly useful to combine with ASGC as will be discussed later. The component functions are orthogonal with respect to the inner product induced by the measure μ ,

$$\int_{\Gamma^N} f_{\mathbf{u}}(\mathbf{Y}_{\mathbf{u}}) f_{\mathbf{v}}(\mathbf{Y}_{\mathbf{v}}) d\mu(\mathbf{Y}) = 0, \quad \text{for } \mathbf{u} \neq \mathbf{v}, \quad (35)$$

and thus the resulting decomposition Eq. (30) is unique for a fixed measure μ . In the next sections, we will present two particularly useful decompositions.

4.1 ANOVA-HDMR

In this case, the measure μ is taken as the ordinary Lebesgue measure $d\mu(\mathbf{Y}) = d(\mathbf{Y}) = \prod_{i=1}^N Y_i$. With this choice, the actions of the projection operators in the ANOVA-HDMR are given by

$$P_{\mathbf{u}}f(\mathbf{Y}_{\mathbf{u}}) := \int_{\Gamma^{N-|\mathbf{u}|}} f(\mathbf{Y}) d\mathbf{Y}_{\mathcal{D}\setminus\mathbf{u}}. \quad (36)$$

More specifically, the first few terms are

$$\begin{aligned} f_0 &= \int_{\Gamma^N} f(\mathbf{Y}) d\mathbf{Y}, \quad f_i(Y_i) = \int_{\Gamma^{N-1}} f(\mathbf{Y}) \prod_{j \neq i} dY_j - f_0 \\ f_{ij}(Y_i, Y_j) &= \int_{\Gamma^{N-2}} f(\mathbf{Y}) \prod_{k \neq i, j} dY_k - f_i(Y_i) - f_j(Y_j) - f_0, \quad \dots \end{aligned} \quad (37)$$

This decomposition is the same as the well-known analysis of variance (ANOVA) decomposition used in statistics. A significant drawback of ANOVA-HDMR is the need to compute the high-dimensional integrals. Even the zeroth-order

component function requires a full-dimensional integration in the space. To circumvent this difficulty, a computationally more efficient Cut-HDMR expansion will be introduced in the following section for the stochastic model representation which is the focus of this paper.

4.2 CUT-HDMR

In this work, the CUT-HDMR is adopted to construct the response surface of the stochastic solution. With this method, the measure μ is chosen as the Dirac measure located at a reference point $\bar{\mathbf{Y}} = (\bar{Y}_1, \bar{Y}_2, \dots, \bar{Y}_N)$, i.e. $d\mu(\mathbf{Y}) = \prod_{i=1}^N \delta(Y_i - \bar{Y}_i) dY_i$. If the HDMR is a converged expansion, the choice of this point does not affect the approximation. In our work, the mean of the random input vector is chosen as the reference point. With this choice, the projections Eq. (32) become

$$P_{\mathbf{u}}f(\mathbf{Y}_{\mathbf{u}}) := f(\mathbf{Y})|_{\mathbf{Y}=\bar{\mathbf{Y}} \setminus \mathbf{Y}_{\mathbf{u}}}, \quad (38)$$

where the notation $\mathbf{Y} = \bar{\mathbf{Y}} \setminus \mathbf{Y}_{\mathbf{u}}$ means that the components of \mathbf{Y} other than those indices that belong to the set \mathbf{u} are set equal to those of the reference point. Equation (38) defines a $|\mathbf{u}|$ -dimensional function where the unknown variables are those dimensions which indices that belong to \mathbf{u} . The component functions of CUT-HDMR are explicitly given as follows [24]:

$$\begin{aligned} f_0 &= f(\bar{\mathbf{Y}}), \quad f_i(Y_i) = f(\mathbf{Y})|_{\mathbf{Y}=\bar{\mathbf{Y}} \setminus Y_i} - f_0 \\ f_{ij}(Y_i, Y_j) &= f(\mathbf{Y})|_{\mathbf{Y}=\bar{\mathbf{Y}} \setminus (Y_i, Y_j)} - f_i(Y_i) - f_j(Y_j) - f_0, \quad \dots \end{aligned} \quad (39)$$

The basic conjecture underlying HDMR is that the component functions arising in typical physical problems will not likely exhibit high-order cooperativity among the input variables such that the significant terms in the HDMR expansion are expected to satisfy the relation: $|\mathbf{u}| \ll N$ for $N \gg 1$ [24,25]. Therefore, it is expected that the HDMR expansion will converge very fast. For most well-defined physical systems, the first- and second-order expansion terms are expected to have most of the impact upon the output and the contribution of higher-order terms would be insignificant. However, the importance of higher-order terms in HDMR is problem-dependent. The exact effect in stochastic space from the input variability is unclear and this will be one of the focus points in this paper.

It is also interesting to note that the CUT-HDMR can be derived from a Taylor expansion at the reference point [33]. The infinite number of terms in the Taylor series are partitioned into finite different groups and each group corresponds to one CUT-HDMR component functions, e.g, the first-order component function $f_i(Y_i)$ is the sum of all the Taylor series terms which contain

and only contain variable Y_i and so on [28]. Any truncated HDMR expansion should provide higher-order accuracy than a truncated Taylor series of the same order.

4.3 Integrating HDMR and ASGC

Although ASGC depends less on dimensionality than the gPC method, it still suffers with increasing number of dimensions (see logarithmic term of the error bound in Eq. (21)). Therefore, for problems with high stochastic dimensionality, to obtain accurate results one needs to use a higher-interpolation level. However, the number of needed points will grow quickly as shown in Fig. 1.

Within the framework of CUT-HDMR, let us rewrite Eqs. (30) and (34) as

$$f(\mathbf{Y}) = \sum_{\mathbf{u} \subseteq \mathcal{D}} f_{\mathbf{u}}(\mathbf{Y}_{\mathbf{u}}) = \sum_{\mathbf{u} \subseteq \mathcal{D}} \sum_{\mathbf{v} \subseteq \mathbf{u}} (-1)^{|\mathbf{u}|-|\mathbf{v}|} f(\mathbf{Y}_{\mathbf{v}})_{\mathbf{Y}=\bar{\mathbf{Y}} \setminus \mathbf{Y}_{\mathbf{v}}}, \quad (40)$$

where we define $f(\mathbf{Y}_{\emptyset}) = f(\bar{\mathbf{Y}})$. Therefore, the N -dimensional stochastic problem is transformed to several lower-order $|\mathbf{v}|$ -dimensional problems $f(\mathbf{Y}_{\mathbf{v}})_{\mathbf{Y}=\bar{\mathbf{Y}} \setminus \mathbf{Y}_{\mathbf{v}}}$ which can be easily solved by the ASGC as introduced in the last section:

$$f(\mathbf{Y}) = \sum_{\mathbf{u} \subseteq \mathcal{D}} \sum_{\mathbf{v} \subseteq \mathbf{u}} (-1)^{|\mathbf{u}|-|\mathbf{v}|} \sum_{\|\mathbf{i}\| \leq N+q} \sum_{\mathbf{j} \in B_{\mathbf{i}}} w_{\mathbf{v}}^{\mathbf{ij}}(\mathbf{x}) \cdot a_{\mathbf{j}}^{\mathbf{i}}(\mathbf{Y}_{\mathbf{v}}), \quad (41)$$

where $\|\mathbf{i}\| = i_1 + \dots + i_{|\mathbf{v}|}$, $w_{\mathbf{v}}^{\mathbf{ij}}(\mathbf{x})$ are the hierarchical surpluses for different sub-problems indexed by \mathbf{v} and $a_{\mathbf{j}}^{\mathbf{i}}(\mathbf{Y}_{\mathbf{v}})$ is only a function of the coordinates which belong to the set \mathbf{v} . It is noted that the interpolation level q may be different for each sub-problem according to their regularity along the particular dimensions which is controlled by the error threshold ε in Algorithm 1.

Interpolation is done quickly here (with no need to search any tables) through simple weighted sum of the basis functions and the corresponding hierarchical surpluses. In addition, it is also easy to extract statistics as introduced in Section 3.2 by integrating directly the interpolating basis functions. Let us denote

$$J_{\mathbf{u}} = \sum_{\mathbf{v} \subseteq \mathbf{u}} (-1)^{|\mathbf{u}|-|\mathbf{v}|} \sum_{\|\mathbf{i}\| \leq N+q} \sum_{\mathbf{j} \in B_{\mathbf{i}}} w_{\mathbf{v}}^{\mathbf{ij}}(\mathbf{x}) \cdot I_{\mathbf{j}}^{\mathbf{i}}, \quad (42)$$

as the mean of the component function $f_{\mathbf{u}}$. Then the mean of the HDMR expansion is simply $\mathbb{E}[f(\mathbf{Y})] = \sum_{\mathbf{u} \subseteq \mathcal{D}} J_{\mathbf{u}}$. To obtain the variance of the solution, we can similarly construct an approximation for u^2 and use the formula $\text{Var}[u(\mathbf{x})] = \mathbb{E}[u^2(\mathbf{x})] - (\mathbb{E}[u(\mathbf{x})])^2$.

Remark 1. It is also possible to use the Smolyak quadrature rule directly to integrate the CUT-HDMR in order to obtain the mean and the variance [37]. However, the method introduced here is much better since it provides a function approximation to the output that can be used as a stochastic reduced-order model [40] with local adaptivity build in its representation.

4.4 The effective dimension of a multivariate stochastic function

Related to HDMR expansions is the concept of the effective dimension of a multivariate function [37,38]. In [37], the authors have discussed it in the case of integration. Here, we extend this concept to a multivariate stochastic function. Let $\hat{f} := \sum_{\mathbf{u} \subseteq \mathcal{D}} |J_{\mathbf{u}}|$ be the sum of all contributions to the mean value, where the operator $|J_{\mathbf{u}}| = |\int f_{\mathbf{u}} dY_{\mathbf{u}}| \leq \|f_{\mathbf{u}}\|_{L_1}$ and thus are related to the L_1 norm[37]. Then, for the proportion $\alpha \in (0, 1]$, the *truncation dimension* is defined as the smallest integer N_t , such that

$$\sum_{\mathbf{u} \subseteq \{1, \dots, N_t\}} |J_{\mathbf{u}}| \geq \alpha \hat{f}, \quad (43)$$

whereas, the *superposition dimension* is defined as the smallest integer N_s , such that

$$\sum_{|\mathbf{u}| \leq N_s} |J_{\mathbf{u}}| \geq \alpha \hat{f}. \quad (44)$$

The superposition dimension is also called the *order* of the HDMR expansion. The effective dimensions in the case of interpolation cannot be defined in a unique manner and their definition is part of the algorithmic approach used.

With the definition of effective dimensions, we can thus truncate the expansion in Eq. (30). In other words, we take only a subset \mathcal{S} of all indices $\mathbf{u} \subseteq \mathcal{D}$. Here, we assume that the set \mathcal{S} satisfies the following admissible condition:

$$\mathbf{u} \in \mathcal{S} \text{ and } \mathbf{v} \subset \mathbf{u} \Rightarrow \mathbf{v} \in \mathcal{S}. \quad (45)$$

This is to guarantee that all the terms can be calculated according to Eq. (34). For example, the set of superposition dimension can be defined as $\mathcal{S}_{N_s} := \{\mathbf{u} \subseteq \mathcal{D} : |\mathbf{u}| \leq N_s\}$ and the set of truncation dimension can be defined as $\mathcal{S}_{N_t} := \{\mathbf{u} \subseteq \{1, \dots, N_t\}\}$.

Therefore, from Section 4.3, we can define an interpolation formula $\mathcal{A}_{\mathcal{S}}f$ for the approximation of f which is given by

$$\mathcal{A}_{\mathcal{S}}f := \sum_{\mathbf{u} \in \mathcal{S}} \mathcal{A}(f_{\mathbf{u}}). \quad (46)$$

It is common to refer to the terms $\{f_{\mathbf{u}} : |\mathbf{u}| = l\}$ collectively as the “order- l terms”. Then the expansion order for the decomposition Eq. (46) is the

maximum of l . Note that the number of collocation points in this expansion is defined as the sum of the number of points for each sub-problem from Eq. (41), i.e. $M = \sum_{\mathbf{v} \in \mathcal{S}} M_{\mathbf{v}}$.

Now, let us consider the approximation error of the truncated HDMR expansion with ASGC used for the component functions in Eq. (46). To this end, we fix $\alpha \in (0, 1]$ and assume that N_s and N_t , the corresponding superposition and truncation dimensions, are known. We define the index set $\mathcal{S}_{N_t, N_s} := \{\mathbf{u} \subseteq \{1, \dots, N_t\}, |\mathbf{u}| \leq N_s\}$. We have the following theorem:

Theorem 1. *Let $\mathcal{S} = \mathcal{S}_{N_t, N_s}$, and let \mathcal{A} be the ASGC interpolant with the same error threshold ε for all the sub-problems. Then:*

$$|f - \mathcal{A}_{\mathcal{S}}f| \leq c(N_s, N_t)\varepsilon + \varepsilon_t, \quad (47)$$

for all $f \in F_N$. Here, the constant $c(N_t, N_s)$ depends on the effective dimensions, but does not depend on the nominal dimension N . ε_t is the truncation error of Eq. (46) according to the definition of effective dimensions.

Proof: The proof of this theorem is similar to that of Theorem 3.3 in [37]. We start with

$$|f - \mathcal{A}_{\mathcal{S}}f| \leq |f - f_{\mathcal{S}}| + |f_{\mathcal{S}} - \mathcal{A}_{\mathcal{S}}f|, \quad (48)$$

where $f_{\mathcal{S}} := \sum_{\mathbf{u} \in \mathcal{S}_{N_t, N_s}} f_{\mathbf{u}}(\mathbf{Y}_{\mathbf{u}})$. The first term on the right hand side is the truncation error and the second term is the interpolation error. According to the definition of effective dimensions, with increasing $\alpha \in (0, 1]$, the approximation approaches the true value. Therefore, for a fixed α , we can denote the truncation error as $|f - f_{\mathcal{S}}| = \varepsilon_t$. From Eq. (34), we have the expression

$$f_{\mathbf{u}} - A(f_{\mathbf{u}}) = \sum_{\mathbf{v} \subseteq \mathbf{u}} (-1)^{|\mathbf{u}| - |\mathbf{v}|} (P_{\mathbf{v}}f - A(P_{\mathbf{v}}f)). \quad (49)$$

According to the ASGC algorithm, it is known that the approximation error is controlled by the error threshold ε . Since we choose the same ε for each sub-problem, we have $|P_{\mathbf{v}}f - A(P_{\mathbf{v}}f)| \leq \varepsilon$ [23].

Therefore, we have

$$\begin{aligned} |f_{\mathcal{S}} - \mathcal{A}_{\mathcal{S}}(f)| &\leq \sum_{\mathbf{u} \in \mathcal{S}} |f_{\mathbf{u}} - A(f_{\mathbf{u}})| \leq \sum_{\mathbf{u} \in \mathcal{S}} \sum_{\mathbf{v} \subseteq \mathbf{u}} |P_{\mathbf{v}}f - A(P_{\mathbf{v}}f)| \\ &\leq \sum_{\mathbf{u} \in \mathcal{S}} \sum_{\mathbf{v} \subseteq \mathbf{u}} \varepsilon = \sum_{k=1}^{N_s} \binom{N_t}{k} \sum_{j=1}^k \binom{k}{j} \varepsilon \leq c(N_t, N_s)\varepsilon, \end{aligned} \quad (50)$$

with the constant $c(N_t, N_s)$ given as [37]

$$c(N_t, N_s) := \sum_{k=1}^{N_s} \binom{N_t}{k} \sum_{j=1}^k \binom{k}{j} \leq \sum_{k=1}^{N_s} \binom{N_t}{k} 2^k \leq 2^{N_s+1} N_t^{N_s},$$

which completes the proof.

Therefore, it is expected that the expansion Eq. (46) converges to the true value with decreasing error threshold ε and increasing number of component functions.

4.5 Adaptive HDMR

In practice, the effective dimensions are not known *a priori*. In order to find the effective dimensions, one needs to compute all 2^N component functions. They were originally defined for the representation of pure mathematical functions [29,37]. However, in our case, calculating effective dimensions is not practical since we need to solve PDEs and thus the computational cost is much higher than that for function evaluation. Note that the total number of component functions for a l -th order expansion is $\sum_{i=0}^l \frac{N!}{i!(N-i)!}$, which increases quickly with the number of dimensions. Therefore, in this section, we would like to develop an adaptive version of HDMR for automatically and simultaneously detecting the truncation and superposition dimensions.

We here assume each component function $f_{\mathbf{u}}$ is associated with a weight $\eta_{\mathbf{u}} \geq 0$, which describes the contribution of the term $f_{\mathbf{u}}$ to the HDMR. Using this information, we then want to automatically determine the optimal index set \mathcal{S} , which consists of two steps.

At first, we try to find the important dimensions, i.e. the truncation dimension. To this end, we always construct the zeroth- and first-order HDMR expansion where the computational cost is affordable even for very high-dimensions. Each first-order component function is only a one-dimensional function and contains information from only one particular dimension. In this case, the weight is defined as:

$$\eta_i = \frac{\|J_{\{i\}}\|_{L_2}}{\|f_0(\mathbf{Y})\|_{L_2}}, \quad (51)$$

where $J_{\{i\}} = \int f_i(Y_i) dY_i$ follows the definition in Eq. (42) and the L_2 norm is defined in the spatial domain in case the output is a vector value. Therefore, this weight measures the relative importance to the reference value from each dimension. Then we define the important dimensions as those whose weights are larger than a predefined error threshold θ_1 . Now, the set \mathcal{D} in Eq. (40) only contains these important dimensions instead of all the dimensions. For

example, if the important dimensions are 1, 3 and 5, then only the higher order terms $\{13\}$, $\{15\}$, $\{35\}$ and $\{135\}$ are considered.

However, not all the possible terms are computed. Instead, we adaptively construct these possible higher-order component functions increasingly from lower-order to higher-order in order to reduce the computational cost in the following way. For each computed higher-order term $f_{\mathbf{u}}$, $|\mathbf{u}| \geq 2$, a weight is also defined as

$$\eta_{\mathbf{u}} = \frac{\|J_{\mathbf{u}}\|_{L_2}}{\left\| \sum_{\mathbf{v} \in \mathcal{S}, |\mathbf{v}| \leq |\mathbf{u}|-1} J_{\mathbf{v}} \right\|_{L_2}}. \quad (52)$$

It measures the relative importance with respect to the sum of current integral value which has already been computed in set \mathcal{S} from the previous order. Similarly, the important component functions are defined as those whose weights are larger than the predefined error threshold θ_1 . We put all the important dimensions and higher-order terms into a set \mathcal{T} , which is called the important set. When adaptively constructing HDMR for each new order, we then only calculate the term $f_{\mathbf{u}}$ whose indices satisfy the admissibility relation Eq. (45)

$$\mathbf{u} \in \mathcal{D} \text{ and } \mathbf{v} \subset \mathbf{u} \Rightarrow \mathbf{v} \in \mathcal{T}. \quad (53)$$

In other words, among all the possible indices, we only want to find the terms which can be computed using the previous known important component functions via Eq. (33). In this way, we try to find those terms which may have significant contributions to the overall expansion while ignoring other trivial terms in order to reduce the computational cost for extremely high-dimensional problems.

Let us denote the order of expansion as p . Furthermore, we also define a relative error ρ of the integral value between two consecutive expansion orders p and $p-1$ as

$$\rho = \frac{\left\| \sum_{|\mathbf{u}| \leq p} J_{\mathbf{u}} - \sum_{|\mathbf{u}| \leq p-1} J_{\mathbf{u}} \right\|_{L_2}}{\left\| \sum_{|\mathbf{u}| \leq p-1} J_{\mathbf{u}} \right\|_{L_2}}. \quad (54)$$

If ρ is smaller than another predefined error threshold θ_2 , the HDMR is regarded as converged and the construction stops.

The above procedure is detailed in Algorithm 2.

It is noted here that we add all the computed indices to set \mathcal{S} even if their weight is below the threshold θ_1 in order to further improve the accuracy since we have already paid the cost to compute them. This is similar idea to that used in the ASGC Algorithm 1 [23].

Algorithm 2 Adaptive construction of the index set \mathcal{S}

Initialize: Let $\mathcal{S} = \{\emptyset\}$, $\mathcal{R} = \{\emptyset\}$ and $\mathcal{T} = \{\emptyset\}$. Set $p = 1$.

Construct the zeroth and first-order component functions:

- Solve each sub-problem using the ASGC method with error threshold ε and add all the indices to \mathcal{S} .
- Compute the weights of each first-order term according to Eq. (51). Add those dimensions which satisfy $\eta \geq \theta_1$ to set \mathcal{T} .

repeat

- $p \leftarrow p + 1$. Construct the set \mathcal{R} whose indices satisfy the admissibility relation Eq. (53) for $|\mathbf{u}| = p$.
- If $\mathcal{R} \neq \{\emptyset\}$, for each index $\mathbf{u} \in \mathcal{R}$, solve the corresponding sub-problem using ASGC with error threshold ε and add all the indices to \mathcal{S} .
- Compute the weight of component functions according to Eq. (52). Add those indices which satisfy $\eta \geq \theta_1$ to set \mathcal{T} and clear set \mathcal{R} .
- Compute the relative error ρ according to Eq. (54).

until $\mathcal{R} = \{\emptyset\}$ or $\rho < \theta_2$;

5 Numerical examples: Flow through random heterogeneous media

In this section, we consider flow through random porous media where the permeability is a random field obtained from the K-L expansion of an exponential covariance function. Through this classical problem, we want to investigate the effects of input variability on the accuracy and convergence of HDMR. The problem is defined as follows:

$$\nabla \cdot \mathbf{u}(\mathbf{x}, \mathbf{Y}) = f(\mathbf{x}), \quad (55)$$

$$\mathbf{u}(\mathbf{x}, \mathbf{Y}) = -K(\mathbf{x}, \mathbf{Y})\nabla p(\mathbf{x}, \mathbf{Y}), \quad (56)$$

where the source/sink term $f(\mathbf{x})$ is taken to be deterministic and $K(\mathbf{x}, \mathbf{Y})$ is the random permeability. The domain of interest is a quarter-five spot problem in a unit square $D = [0, 1]^2$. Flow is driven by an injection well at the left bottom corner of the domain and a production well at the top right corner. A mixed finite element method is utilized to solve the forward problem [21].

The log-permeability is taken as zero mean random field with a separable exponential covariance function

$$\text{Cov}(\mathbf{x}, \mathbf{y}) = \sigma^2 \exp\left(-\frac{|x_1 - y_1|}{L} - \frac{|x_2 - y_2|}{L}\right), \quad (57)$$

where L is the correlation length and σ is the standard deviation of the random

field. The K-L expansion is used to parameterize the field as

$$\mathbf{Y}(\omega) = \log(K(\omega)) = \sum_{i=1}^N \sqrt{\lambda_i} \phi_i(\mathbf{x}) Y_i, \quad (58)$$

where the eigenvalues $\lambda_i, i = 1, 2, \dots$, and their corresponding eigenfunctions $\phi_i, i = 1, 2, \dots$, can be determined analytically as discussed in [1,5]. The Y_i are assumed as i.i.d. uniform random variables on $[-1, 1]$.

In order to investigate the accuracy and applicability of the proposed HDMR approach, we design a series of numerical runs with different correlation length L and various degrees of spatial variability σ^2 . The first three cases aim to investigate the effects of correlation lengths ($L = 1.0, 0.5$ and 0.25) on the proposed approach. In these cases, the degree of spatial variability is kept at $\sigma^2 = 1.0$, which corresponds to a moderately high variability. The next three cases are compared against case 3 when $L = 0.25$ to examine the impact of the log-permeability variability ($\sigma^2 = 0.01, 0.25$ and 2.0) ranging from very low to extremely high variability. Monte Carlo simulations are conducted for the purpose of comparison. For each case, the reference solution is taken from 10^6 MC samples and all errors are defined as normalized L_2 errors. Due to the chosen boundary conditions, for each case, the obtained mean value compared very well with the corresponding MC results and therefore we will focus our discussion only on the standard deviation. In all cases, the threshold θ_2 for the relative error is fixed at $\theta_2 = 10^{-4}$.

Let us first determine the stochastic dimension of our example cases. The eigenvalues and the sum of the eigenvalues as a function of the number of terms included are illustrated in Fig. 3 with three different correlation lengths for the case $\sigma^2 = 1.0$. The corresponding eigenfunctions are shown in Fig. 4. Based on these figures, the K-L expansions are truncated after 33, 108 and 500 terms, respectively for $L = 1.0, 0.5, 0.25$, which represents $\approx 95\%$ percent of the total variance of the exponential covariance function. The truncation level for the expansion does not change for a fixed correlation length. Therefore, in all cases, the number of stochastic dimensions is $N = 33, 108$ and 500 , respectively for $L = 1.0, 0.5$ and 0.25 .

5.1 Effect of correlation length

We fix $\sigma^2 = 1.0$ and consider three different correlation lengths at $L = 1.0, 0.5$ and 0.25 . In this way, the input variability is fixed and the change of correlation length adjusts the weights of each random dimension. Thus, we want to investigate the effect of the smoothness of the stochastic space on the accuracy of the HDMR expansion.

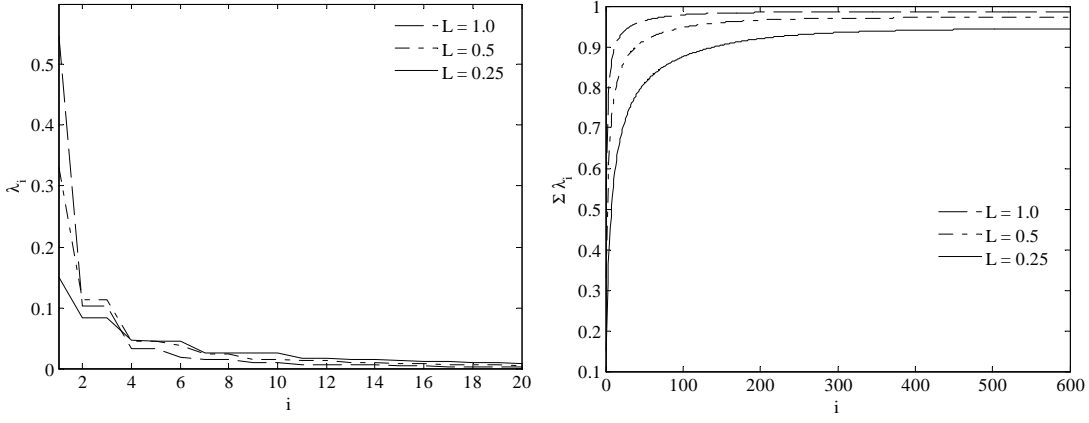


Fig. 3. Series of eigenvalues and their finite sums for three different correlation lengths at $\sigma^2 = 1.0$.

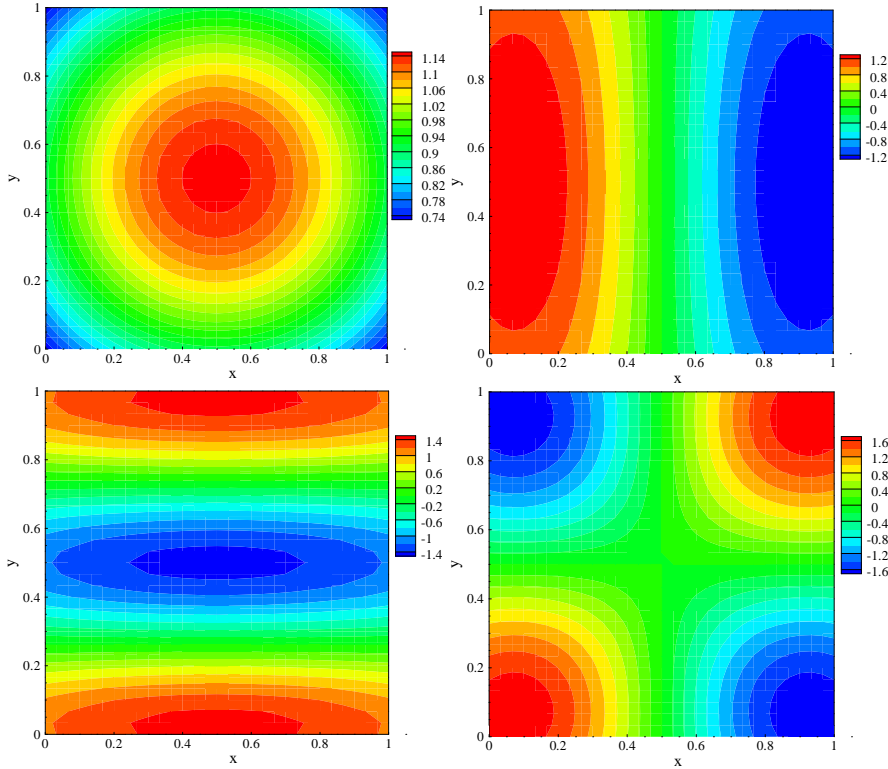


Fig. 4. Four different eigenfunctions for $L = 1.0$ and $\sigma^2 = 1.0$. Top left: ϕ_1 ; Top right: ϕ_2 ; Bottom left: ϕ_5 ; Bottom right: ϕ_6 .

We decrease ε and θ_1 simultaneously until the L_2 normalized errors reach the order of $\mathcal{O}(10^{-3})$. It is interesting to note that these computed errors are achieved with the same $\varepsilon = 10^{-6}$ and $\theta_1 = 10^{-4}$ for all three correlation lengths. In Fig. 5, we compare the standard deviation of the v velocity-component along the line $y = 0.5$ with the results from the MC simulation. It is seen that the two results compare extremely well, where the errors are 1.46×10^{-3} , 1.19×10^{-3} and 1.39×10^{-3} , respectively for $L = 1.0$, $L = 0.5$

and $L = 0.25$.

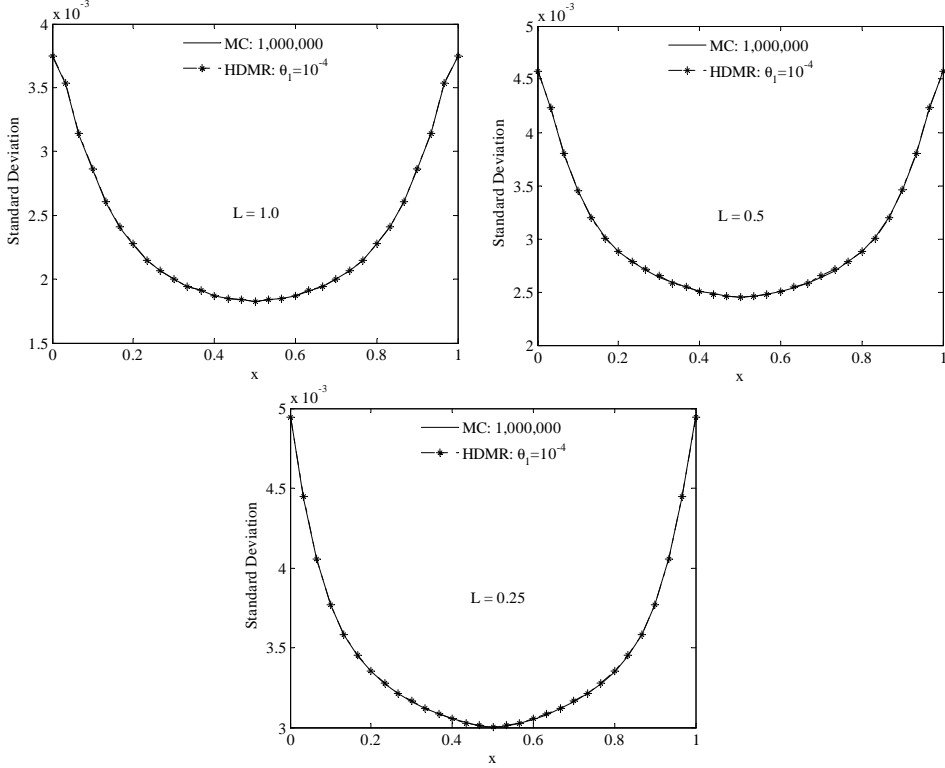


Fig. 5. Standard deviation of the v velocity-component along the cross section $y = 0.5$ for different correlation lengths where $\sigma^2 = 1.0$, $\varepsilon = 10^{-6}$ and $\theta_1 = 10^{-4}$.

To investigate the convergence of HDMR, we fix $\varepsilon = 10^{-6}$ while varying θ_1 . The PDFs of the v velocity-component at point $(0, 0.5)$, where the standard deviation is large as in Fig. 5, are shown in Fig. 6. Each PDF is generated by plotting the kernel density estimate of 10000 output samples through sampling the input space and computing the output value through the HDMR approximation. When $\theta_1 = 10^{-2}$, the weights of all first-order terms are smaller than the threshold and thus there are no higher-order terms. It is seen that the results from only the first-order expansion are not accurate in all three cases. This may be explained intuitively as follows. The spatial variability σ^2 determines the total input variability, which further determines the interactive effects between the input variables. The larger the input variability is, the stronger the interactive effects are. The role of HDMR component functions is to capture these input effects upon the output. In other words, the number of component functions needed depends on the input variability. The higher the input variability is, the more component functions are needed for a fixed stochastic dimension. For low input variability, even first-order expansion may be accurate enough no matter what the stochastic dimension is. In our case, $\sigma^2 = 1.0$ represents a rather high input variability. Higher-order terms are therefore needed to capture these effects whereas only first-order terms are not enough. By decreasing θ_1 , more dimensions whose weights defined in Eq. (51)

are larger than θ_1 become important and thus more second-order terms appear. The number of component functions are 287, 889 and 2271 while for the full second-order expansion they are 562, 5887 and 125251, respectively. Thus, the advantage of using adaptive HDMR is obvious, especially for $N = 500$. As expected, all the results converge to those obtained from the MC simulation with decreasing θ_1 . The accuracy of the PDFs indicate that the corresponding HDMR approximations are indeed very accurate. Therefore, we can obtain any statistic from this stochastic reduced-order model, which is an advantage of the current method over the naive MC method.

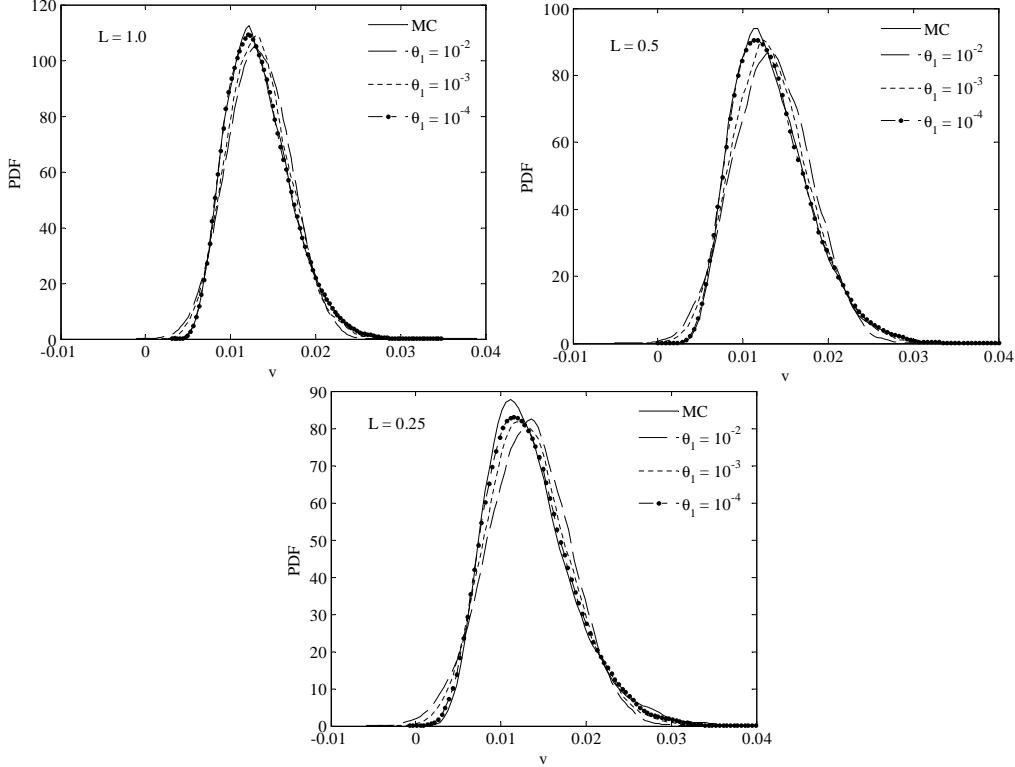


Fig. 6. PDF of v velocity-component at point $(0, 0.5)$ for different correlation lengths, where $\sigma^2 = 1.0$ and $\varepsilon = 10^{-6}$.

The convergence of the L_2 normalized error with respect to the total number of collocation points is shown in Fig. 7 by fixing $\theta_1 = 10^{-4}$. The error plots are obtained by decreasing the threshold ε used in the ASGC. Although different correlation lengths result in different truncated stochastic dimensions from the K-L expansion, it is interesting to note that we still have algebraic convergence rates and they are nearly the same for all three cases. This may be explained using Theorem 1. The input variability is the same and so is the superposition dimension. Thus, the constant in Eq. (47,) which only depends on the effective dimensions, is nearly the same. In addition, the error in Eq. (47) exhibits a linear dependence on the threshold ε and as we know the convergence rate of the sparse grid collocation method is algebraic [17,23]. Thus, the convergence plot here indeed exhibits algebraic rate as indicated from Theorem 1.

In order to further verify the results discussed in this section, we investigate the effect of the spatial variability in the next section.

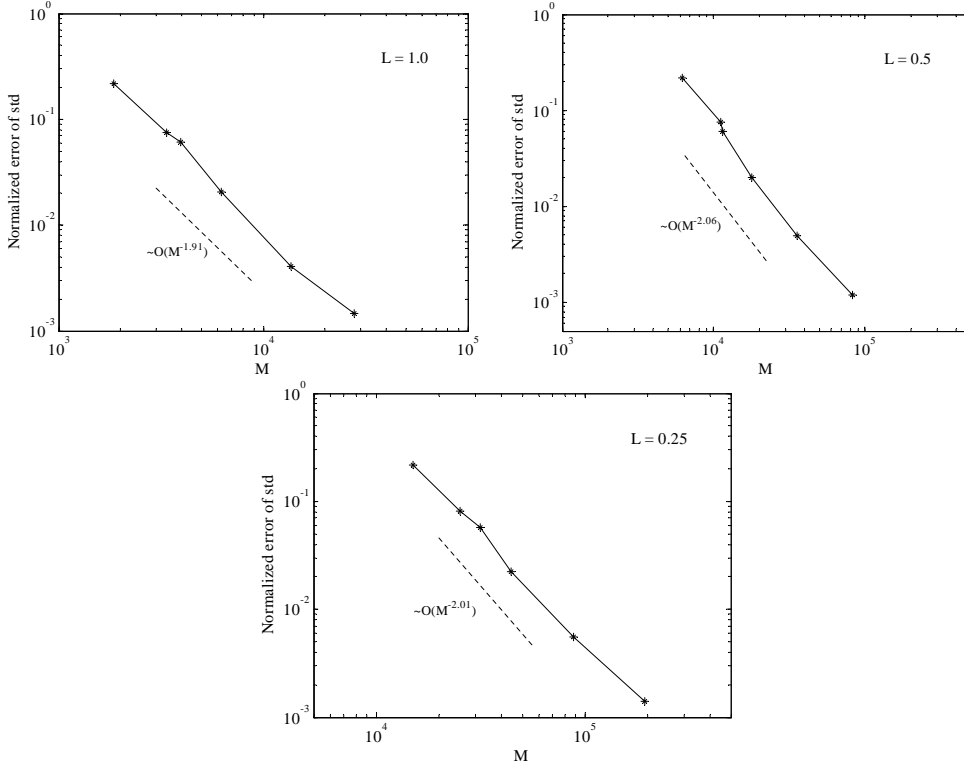


Fig. 7. Convergence of the L_2 normalized errors of the standard deviation of the v velocity-component for different correlation lengths, where $\sigma^2 = 1.0$ and $\theta_1 = 10^{-4}$.

5.2 Effect of the spatial variability σ^2

In this section, we fix the correlation length at $L = 0.25$ such that the weight of each dimension from the K-L expansion is nearly the same. Then we explore the effects of the spatial variability σ^2 , from very small variability $\sigma^2 = 0.01$ to very high variability $\sigma^2 = 2.0$. The number of stochastic dimensions is $N = 500$.

Fig. 8 compares the standard deviation of the v velocity-component along the line $y = 0.5$ with the results obtained from the MC simulation. Again, we obtain very good comparison where the errors are 8.08×10^{-4} , 7.37×10^{-4} and 2.86×10^{-3} for $\sigma^2 = 0.01$, $\sigma^2 = 0.25$ and $\sigma^2 = 2.0$, respectively. Comparing with the the result when $\sigma^2 = 1.0$, it can be seen that the error in standard deviation increases with increasing of the input variability. However, we can still obtain an acceptable accuracy even when the spatial variability is as high as $\sigma^2 = 2.0$. It is interesting to note that the threshold ε needed to achieve the desired accuracy is smaller for $\sigma^2 = 0.01$ and 0.25 than for $\sigma^2 = 1.0$. This is due to the small correlation length and low input variability which results in a rather

smooth stochastic space such that the hierarchical surpluses decrease very fast. Therefore, we need a much smaller ε to trigger the adaptivity otherwise the refinement of ASGC for each sub problem stops earlier. This also shows the ability of ASGC to detect the smoothness of the stochastic space. The increase of the spatial variability also results in the increase of the magnitude of the standard deviation from $\sigma^2 = 0.01$ to $\sigma^2 = 2.0$ in Fig. 8, i.e. increasing of the variability in the solution.

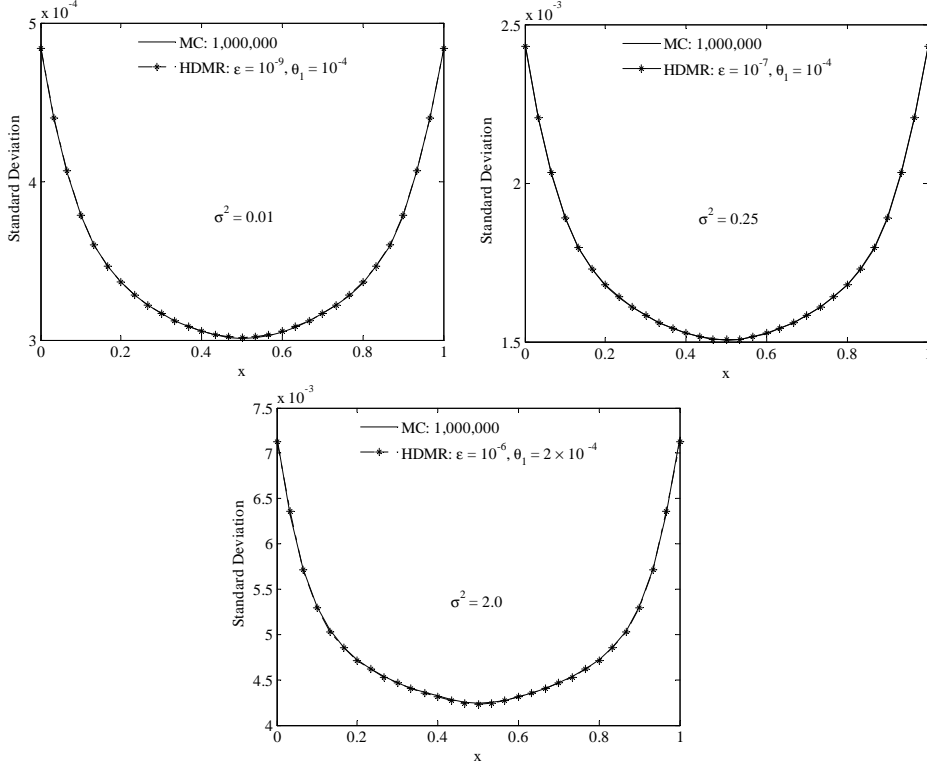


Fig. 8. Standard deviation of the v velocity-component along the cross section $y = 0.5$ for different σ^2 , where $L = 0.25$ and $N = 500$.

Similarly, the convergence of the corresponding PDFs is given in Fig. 9. For the case $\sigma^2 = 0.01$, we show the convergence with respect to ε instead. This is because the first-order expansion is accurate enough to represent the solution due to the low input variability. Even when the value of θ_1 is as small as 10^{-4} , the weights of all the first-order terms from Eq. (51) are still smaller than the threshold. Therefore, there are no second-order terms. Due to the small variability, even a smaller ε can give us a very accurate result as shown in the figure. Compared with Fig. 6, although second-order terms are still needed for the cases $\sigma^2 = 0.25$ and 2.0 , the PDFs from the first-order terms are not apart from the MC results for the cases $\sigma^2 = 0.25$ and $\theta_1 = 10^{-2}$ when the input variability is moderate. On the other hand, for $\sigma^2 = 2.0$, the result from the first-order HDMR expansion ($\theta_1 = 10^{-2}$) deviates significantly from that of the MC results. Indeed, comparing all four cases when $L = 0.25$, it is clear that the PDFs from the first-order expansion deviate gradually from

the MC results with increasing input variability σ^2 . This reflects that the interactive effects become significant and therefore more higher-order terms are needed to capture these effects. The improvement of the results is obvious as more terms are included with decreasing θ_1 . This numerically verifies our previous discussion that the number of component functions needed depends on the input variability. There are 501, 879 and 2271 component functions for $\sigma^2 = 0.01, 0.25$ and 2.0 , respectively. Correspondingly, the total number of collocation points are 9337, 74127, and 249329.

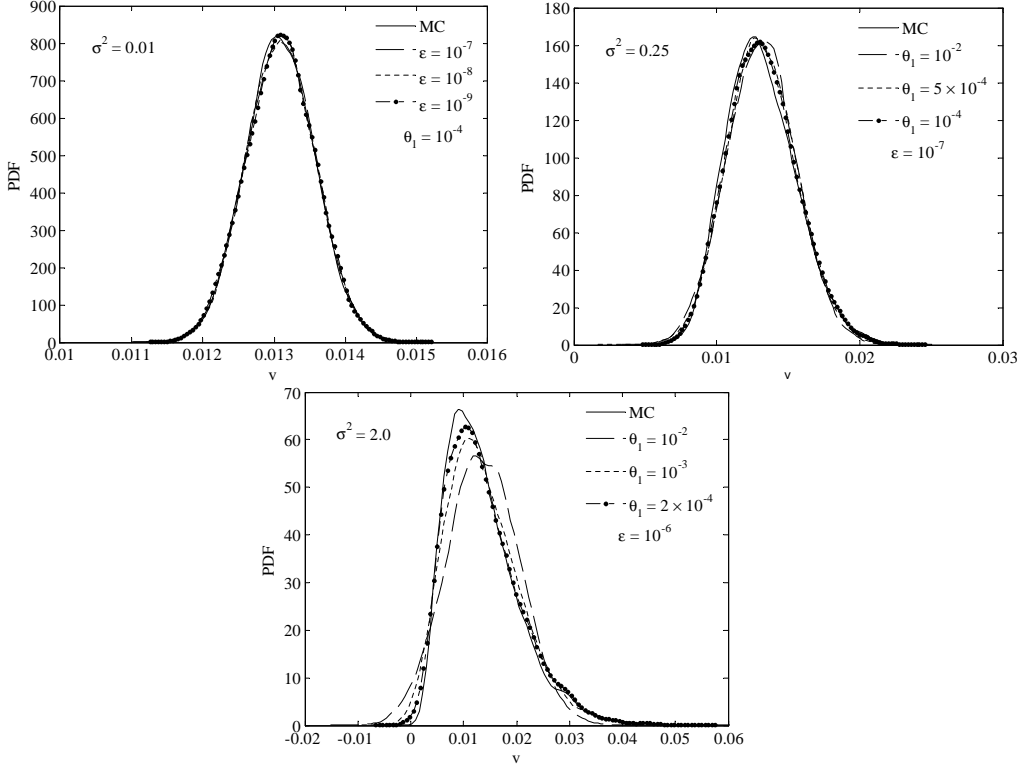


Fig. 9. PDF of the v velocity-component at point $(0, 0.5)$ for different σ^2 , where $L = 0.25$ and $N = 500$.

The convergence of the L_2 normalized error with respect to the total number of collocation points is shown in Fig. 7 by decreasing ϵ in the ASGC. As expected, the convergence rates deteriorate with increasing σ^2 . For $\sigma^2 = 0.01$, the convergence rate is nearly of the order of $\mathcal{O}(M^{-2.87})$. This is because first-order HDMR expansion is used and the number of collocation points used in the first-order terms is much lower than that in higher-order terms. The convergence rate for the case $\sigma^2 = 2.0$ is the lowest among all the cases examined so far. However, it is still better than the theoretic MC rate $\mathcal{O}(M^{-0.5})$ and the results compare well with that of MC. Comparing all four cases when $L = 0.25$, it is seen that although the stochastic space is smooth, the convergence rate still decreases with increasing spatial variability. Thus, as discussed before, the number of component functions needed for a fixed stochastic dimension depends more on the input variability than the smoothness of the

stochastic space. This provides us a very useful guideline to set up the parameters when applying HDMR to realistic stochastic problems. On the other hand, the regularity of the stochastic space can be effectively resolved with the ASGC method. The proposed method is indeed a very powerful and versatile method to address stochastic PDE problems.

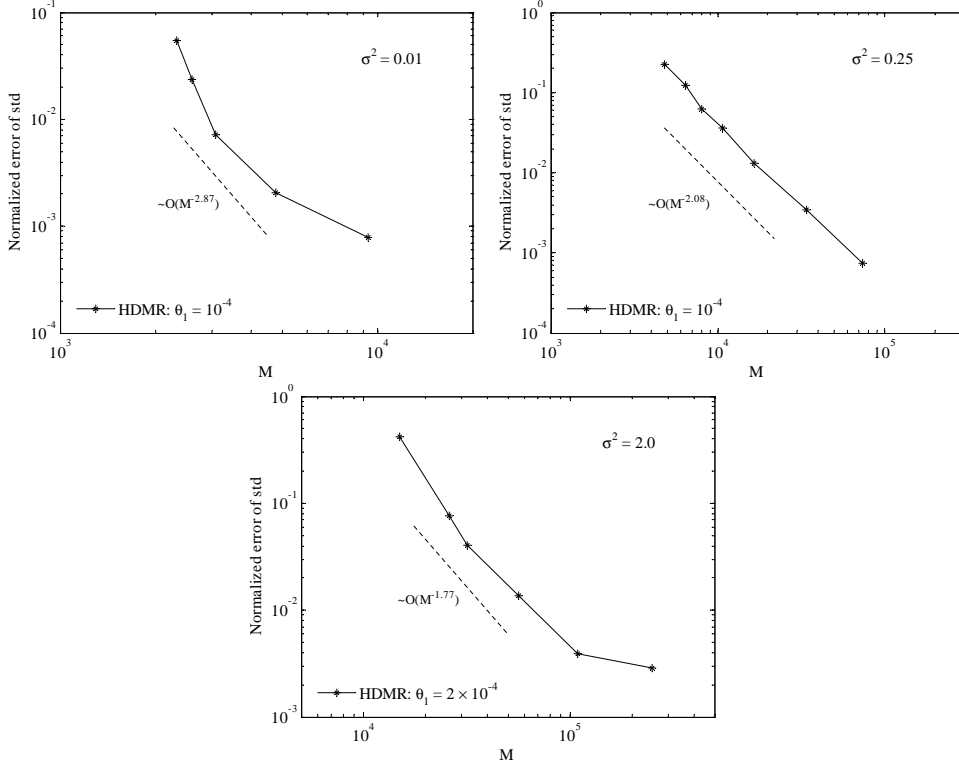


Fig. 10. Convergence of the L_2 normalized errors of standard deviation of the v velocity-component for different σ^2 , where $L = 0.25$.

Finally, it is emphasized here that using the ASGC or CSGC methods alone as in [23] to solve these high-dimensional problems is not feasible due to the following two reasons. At first, the number of needed collocation points is significant for such high-dimensional cases and the convergence rate is very small due to the logarithmic term shown in the error estimation. For example, for $N = 500$, the number of points is 167169001 for a third-level interpolation. Secondly, there is a need for large memory storage to store all the high-dimensional multi-indices. Therefore, we are not able to compare the results shown in this paper with results that can be obtained directly from the ASGC. However, through the numerical examples, it is shown that the method presented here is indeed a useful tool for solving high-dimensional stochastic problems.

6 Conclusions

In this paper, a novel adaptive dimensional stochastic model representation technique for solving high-dimensional SPDEs is introduced. This method applies HDMR in the stochastic space and decomposes the original N -dimensional problem into several low-dimensional sub-problems. This has been shown to be more efficient than solving the N -dimensional problem directly. Each sub-problem is solved using ASGC, where a proper error indicator is introduced to adaptively refine locally the collocation points.

Numerical examples have been conducted to verify the accuracy and efficiency of the proposed method. The numerical examples show that the number of component functions needed in the HDMR expansion for a fixed stochastic dimension depends more on the input variability than the smoothness of the stochastic space no matter how many stochastic dimensions there are. Although, in general, second-order expansion is enough to capture all the input uncertainty, the number of component functions increases quickly with the dimension. It is impossible to calculate all the second-order terms in the case of extremely high-stochastic dimension. However, by using the adaptive version of HDMR, we can effectively solve the problem within a desired accuracy even for high-dimensional high input variability problem. On the other hand, for small variability, first-order expansion is accurate enough. Therefore, the HDMR is quite suitable in most real engineering applications for simulating high-dimensional stochastic problems in the area of uncertainty quantification where the correlation length is small and the input variability is generally large and solving the N -dimensional problem directly by ASGC or CSGC is not feasible. It is also shown that the convergence rate of the proposed method is even better than that of MC.

Finally, we note that the proposed method is more computationally efficient than the previous collocation method since it requires less memory storage and avoids the heavy surplus calculation for really high-dimensional problems. However, we note that this method may not be of practical utility for interpolating arbitrary mathematical functions of multiplicative nature (see e.g. [41]) where all 2^N component functions might be required.

Acknowledgements

This research was supported by the Computational Mathematics program of AFOSR (grant F49620-00-1-0373) and by the Computational Mathematics program of the NSF (award DMS-0809062).

References

- [1] R. Ghanem, P. D. Spanos, *Stochastic Finite Elements: A Spectral Approach*, Springer - Verlag, New York, 1991.
- [2] B. Ganapathysubramanian, N. Zabaras, Modeling diffusion in random heterogeneous media: Data-driven models, stochastic collocation and the variational multiscale method, *Journal of Computational Physics* 226 (2007) 326–353.
- [3] B. Ganapathysubramanian, N. Zabaras, A non-linear dimension reduction methodology for generating data-driven stochastic input models, *Journal of Computational Physics*, 227 (2008) 6612–6637.
- [4] D. Zhang, *Stochastic methods for flow in porous media: Coping with uncertainties*, Academic Press, San Diego, CA, 2002.
- [5] D. Zhang, Z. Lu, An efficient, high-order perturbation approach for flow in random porous media via Karhunen-Loève and polynomial expansions, *J. Comput. Phys.* 194 (2004) 773–794.
- [6] Z. Lu, D. Zhang, A comparative study on flow in uncertainty quantification for flow in randomly heterogeneous media using Monte Carlo simulations and conventional and KL-based moment-equation approaches, *SIAM J. Sci. Comput.* 26 (2004) 558–577.
- [7] D. Xiu, G. E. Karniadakis, The Wiener-Askey polynomial chaos for stochastic differential equations, *SIAM J. Sci. Comput.* 24 (2002) 619–644.
- [8] R. Ghanem, Probabilistic characterization of transport in heterogeneous media, *Comput. Methods Appl. Mech. Engrg.* 158 (1998) 199–220.
- [9] D. Xiu, G. E. Karniadakis, Modeling uncertainty in steady state diffusion problems via generalized polynomial chaos, *Comput. Methods Appl. Mech. Engrg.* 191 (2002) 4927-4948.
- [10] D. Xiu, G. E. Karniadakis, A new stochastic approach to transient heat conduction modeling with uncertainty, *Int. J. Heat Mass Transfer* 46 (2003) 4681-4693.
- [11] B. Velamuri Asokan, N. Zabaras, A stochastic variational multiscale method for diffusion in heterogeneous random media, *J. Comp. Physics* 218 (2006) 654–676.
- [12] X. Ma, N. Zabaras, A stabilized stochastic finite element second-order projection method for modeling natural convection in random porous media, *J. Comp. Physics*, 227 (2008) 8448-8471.
- [13] I. Babuska, R. Tempone, G. E. Zouraris, Galerkin finite elements approximation of stochastic finite elements, *SIAM J. Numer. Anal.* 42 (2004) 800–825.
- [14] D. Xiu, J. S. Hesthaven, High order collocation methods for the differential equation with random inputs, *SIAM J. Sci. Comput.* 27 (2005) 1118–1139.

- [15] D. Xiu, Efficient Collocational Approach for Parametric Uncertainty Analysis, *Communications In Computational Physics* 2 (2007) 293–309.
- [16] I. Babuska, F. Nobile, R. Tempone, A stochastic collocation method for elliptic partial differential equations with random input data, *SIAM J. Numer. Anal.* 45 (2007) 1005–1034.
- [17] F. Nobile, R. Tempone, C. Webster, A sparse grid collocation method for elliptic partial differential equations with random input data, *SIAM J. Numer. Anal.* 45 (2008) 2309–2345.
- [18] B. Ganapathysubramanian, N. Zabaras, Sparse grid collocation schemes for stochastic natural convection problems, *J. Comp. Physics* 225 (2007) 652–685.
- [19] F. Nobile, R. Tempone, C. Webster, An anisotropic sparse grid collocation method for elliptic partial differential equations with random input data, *SIAM J. Numer. Anal.* 46 (2008) 2411–2442.
- [20] S. Smolyak, Quadrature and interpolation formulas for tensor product of certain classes of functions, *Soviet Math. Dokl.* 4 (1963) 240–243.
- [21] B. Ganapathysubramanian, N. Zabaras, A stochastic multiscale framework for modeling flow through heterogeneous porous media, *Journal of Computational Physics*, 228 (2009) 591–618.
- [22] B. Ganis, H. Klie, M. Wheeler, T. Wildey, I. Yotov, D. Zhang, Stochastic collocation and mixed finied elements for flow in porous media, *Comput. Methods Appl. Mech. Engrg.*, 197 (2008) 3547–3559.
- [23] X. Ma, N. Zabaras, An adaptive hierarchical sparse grid collocation method for the solution of stochastic differential equations, *Journal of Computational Physics*, 228 (2009) 3084–3113.
- [24] H. Rabitz, O. F. Alis, J. Shorter, K. Shim, Efficient input-output model representations, *Computer Physics Communications* 117 (1999) 11–20.
- [25] H. Rabitz, O. F. Alis, General foundations of high-dimensional model representations, *Journal of Mathematical Chemistry*, 25 (1999) 197–233.
- [26] O. F. Alis, H. Rabitz, Efficient implementation of high dimensional model representations, *Journal of Mathematical Chemistry*, 29 (2001) 127–142.
- [27] S. W. Wang, H. Levy II, G. Li, H. Rabitz, Fully equivalent operational models for atomspheric chemical kinetics within global chemistry-transport models, *Journal of Geophysical Research*, 104 (1999) 30417–30426.
- [28] G. Li, C. Rosenthal, H. Rabitz, High dimensional model representation, *Journal of Physical Chemistry A*, 105 (2001) 7765–7777.
- [29] I. M. Sobol, Theorems and examples on high dimensional model representation, *Reliability Engineering and System Safety*, 79 (2003) 187–193.

- [30] G. Li, S. W. Wang, H. Rabitz, S. Wang, P. Jaffe, Global uncertainty assessments by high dimensional model representations (HDMR), *Chemical Engineering Science*, 57 (2002) 4445–4460.
- [31] S. Balakrishnan, A. Roy, M. G. Ierapetritou, G. P. Flach, P. G. Georgopoulos, A comparative assessment of efficient uncertainty analysis techniques for environmental fate and transport models: application to the FACT model, *Journal of Hydrology*, 307 (2005) 204-281.
- [32] S. Rahman, H. Xu, A univariate dimension-reduction method for multi-dimensional integration in stochastic mechanics, *Probabilistic Engineering Mechanics*, 19 (2004) 393–408.
- [33] H. Xu, S. Rahman, A generalized dimension-reduction method for multidimensional integration in stochastic mechanics, *Int. J. Numer. Meth. Engng*, 61 (2004) 1992-2019
- [34] H. Xu, S. Rahman, Decomposition methods for structural reliability analysis, *Probabilistic Engineering Mechanics*, 20 (2005) 239–250.
- [35] S. Rahman, A dimensional decomposition method for stochastic fracture mechanics, *Engineering Fracture Mechanics*, 73 (2006) 2093–2109.
- [36] R. Chowdhury, B. N. Rao, A. M. Prasad, High-dimensional model representations for structural reliability analysis, *Commun. Numer. Meth. Engng*, DOI: 10.1002/cnm.1118, 2009.
- [37] M. Griebel, M. Holtz, Dimension-wise integraton of high-dimensional functions with applications to finance, *INS preprint NO. 0809*, November 2008.
- [38] F. Kuo, I. Sloan, G. Wasilkowski, and H. Woźniakowski, On the decompositions of multivariate functions, *Technical report*, University of New South Wales, 2008
- [39] B. Oksendal, *Stochastic Differential Equations: An introduction with applications*, Springer-Verlag, New York, 1998.
- [40] X. Ma, N. Zabararas, An efficient Bayesian inference approach to inverse problems based on adaptive sparse grid collocation method, *Inverse Problems*, 25 (2009) 035313 (27pp).
- [41] A. GENZ, A package for testing multiple integration subroutines, in *Numerical Integration: Recent Developments, Software and Applications*, 1987, pp. 337-340.